

Research Article

Epitope Mapping of *Senecavirus A* 3A Protein Using Monoclonal Antibodies

Liang Meng¹, Xiao-Xiao Tian,¹ Xu-Yan Xiang,¹ Xin-Yu Qi,¹ Han-Rong Zhou,¹ Pei-Yu Xiao,¹ Tong-Qing An,^{1,2} Fan-Dan Meng¹ and Hai-Wei Wang¹

¹State Key Laboratory for Animal Disease Control and Prevention, Harbin Veterinary Research Institute, The Chinese Academy of Agricultural Sciences, Harbin 150069, China

²Heilongjiang Provincial Key Laboratory of Veterinary Immunology, Harbin 150069, China

Correspondence should be addressed to Fan-Dan Meng; mengfandan@caas.cn and Hai-Wei Wang; wanghaiwei@caas.cn

Received 27 November 2024; Accepted 11 April 2025

Academic Editor: Zongfu Wu

Copyright © 2025 Liang Meng et al. Transboundary and Emerging Diseases published by John Wiley & Sons Ltd. This is an open access article under the terms of the Creative Commons Attribution License, which permits use, distribution and reproduction in any medium, provided the original work is properly cited.

Senecavirus A (SVA), an emerging pathogen causing vesicular disease in pigs, poses a significant threat to the swine industry. The nonstructural protein 3A of SVA plays an essential role in the viral replication cycle. In this study, we immunized mice with the prepared SVA 3A protein and produced two monoclonal antibodies (mAbs), AG4 and 2F3. MAb AG4 showed specific reactivity to the linear and conformational 3A protein, whereas mAb 2F3 did not recognize linear epitope of 3A protein. Through truncated 3A protein expression and alanine mutation analysis, we identified ¹SPNEND⁶ as the minimal motif recognized by mAb AG4, with Asn³ being the critical residue. Additionally, we demonstrated that mAb 2F3 failed to recognize the SVA mutant with the ⁷⁵QEETEG⁸⁰ deletion in 3A protein, indicating that ⁷⁵QEETEG⁸⁰ constitutes an essential epitope for mAb 2F3. Further deletion analysis confirmed that ⁷⁵QE⁷⁶ is the crucial motif for mAb 2F3 recognition. Moreover, we found that ¹SPNEND⁶ and ⁷⁵QEETEG⁸⁰ are highly conserved among different SVA strains and are exposed on the surface of the 3A protein. This study contributes to further explore the function of SVA 3A protein and develop diagnostic tools for SVA detection.

Keywords: 3A protein; epitope; monoclonal antibody; *Senecavirus A*

Summary

- Since its discovery in 2002, *Senecavirus A* (SVA) has disseminated extensively across numerous countries. Despite its widespread occurrence, no commercial vaccines are currently available against SVA.
- The 3A protein, known to elicit robust and long-lasting antibody responses in vivo, has been identified as an ideal diagnostic target. Additionally, 3A plays a crucial role in the viral replication cycle.
- We obtained two monoclonal antibodies (mAbs) against the 3A protein and identified the B cell epitopes.
- These findings can help us understand the 3A protein's function in viral replication and develop diagnostic tools.

1. Introduction

Senecavirus A (SVA), also known as *Seneca Valley virus* (SVV), is the sole member of the genus *Senecavirus* within the family Picornaviridae [1]. SVA infection in swine causes vesicular lesions and ulcerations, which clinically indistinguishable from other vesicular diseases, including foot-and-mouth disease (FMD) and vesicular exanthema of swine (VES), thereby complicating diagnosis [2–4]. Since the initial report of an SVA epidemic in Canada in 2007, the SVA has spread rapidly to the United States, Brazil, Thailand, Vietnam, China, and several other countries [5–10], posing a significant risk to the global swine industry.

The genome of SVA is characterized by a single-stranded, positive-sense RNA ~7200 nucleotides in length, comprising a

sequences are listed in Table S1. The recombinant truncated proteins were expressed in *E. coli* BL21 (DE3). These recombinant truncated proteins were then used to map the epitopes of mAbs by Western blotting.

2.7. Construction and Rescue of Epitope-Deleted Viruses. Primers were designed based on the gene sequence of the SVA/HLJ/CHA/2016 strain (Table S2). These primers were used to amplify different epitope deletion fragments, which were cloned into the SVA-I212V/S460L infectious clone backbone through homologous recombination. The recombinant clones were designated pSVA- Δ 3A(3-8), pSVA- Δ 3A(75-80), and pSVA Δ 3A(77-86).

BHK-21 cells in 6-well plates were transfected with the constructed clones using Lipofectamine 3000, following the manufacturer's instructions (Life Technologies, NY, USA). The cells were monitored daily for cytopathic effect (CPE) observation. Epitope deletion viruses were harvested once significant CPE was observed. These rescued viruses were serially passaged 12 times in BHK-21 cells, and the stability was confirmed by sequencing the 3A region.

2.8. Replication Dynamics of Epitope Deletion Virus. BHK-21 cells were seeded in 6-well plates until the cells reached 80% confluence and then infected with either wild-type virus or epitope-deleted virus at an MOI of 0.1 to assess viral replication dynamics. After a 1-h incubation at 37°C, the plates were washed three times with PBS and cultured in DMEM with 2% FBS. Samples were harvested at various time points, and viral titers were determined using the 50% tissue culture infective dose (TCID₅₀) assay. TCID₅₀ values were calculated using the Reed–Muench method.

2.9. Viral Plaque Assay. BHK-21 cells were seeded in 6-well tissue culture plates until cell monolayers reached 100% confluency and then infected with 10-fold serial dilutions of SVA-WT and rSVA - Δ 3A(75-80). After a 1-h incubation at 37°C, the infected cells were washed three times with PBS to remove unbound virus particles and then overlaid with DMEM supplemented with 2% FBS and 5% methylcellulose. When plaques were observed, the DMEM and methylcellulose overlay was carefully removed. The cells were washed thrice with PBS and stained with crystal violet.

2.10. Biological Information Analysis of 3A. The secondary structure and epitopes of the SVA 3A protein were predicted and analyzed using the online software suite PSIPRED (<http://bioinf.cs.ucl.ac.uk/psipred/>) and Bepipred (<https://services.healthtech.dtu.dk/services/BepiPred-3.0/>). Concurrently, the surface accessibility, hydrophilicity/hydrophobicity, and antigenic index of the 3A protein were evaluated using the DNASTAR Protean software. Homology modeling for the 3A protein was conducted using the I-TASSER server to provide a structural framework for further analysis. Comparative analysis of the 3A amino acid sequences across various SVA isolates was performed using MEGA 7.0 software.

2.11. Statistical Analysis. All experiments were set up with three replicates, and each experiment was independently repeated at least three times. Statistical analysis was

conducted using two-way analyses of variance with GraphPad Prism 8.0 software. A *p* value of less than 0.05 for each test was considered statistically significant, and significant differences between groups are indicated by ****p*<0.001, ***p*<0.01, and **p*<0.05.

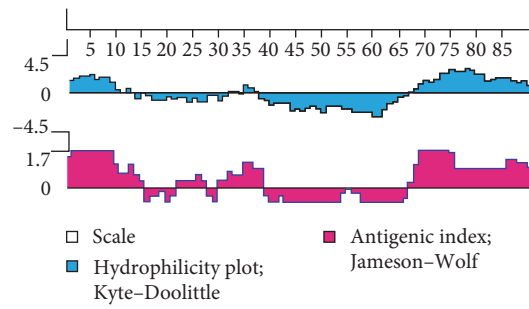
3. Results

3.1. A Protein Expression and Purification. In general, the antigenicity of a protein is mainly determined by the hydrophilicity, surface accessibility, and flexibility of its surface amino acid residues. Hydrophilic regions and random coil regions are more likely to be epitopes due to their high surface accessibility and flexibility [19]. We systematically evaluated the immunogenic potential of 3A protein by comprehensively analyzing its antigenic index, hydrophilicity, and secondary structure composition. Prediction analysis showed that the 3A protein consists of 59% alpha-helix region and 41% random coils (Figure 1B) and that the amino and carboxyl termini of the 3A protein exhibited high antigenicity and hydrophilicity (Figure 1A). The results showed that the 3A protein had good immunogenicity, and the epitopes were mainly concentrated in the amino and carboxyl termini.

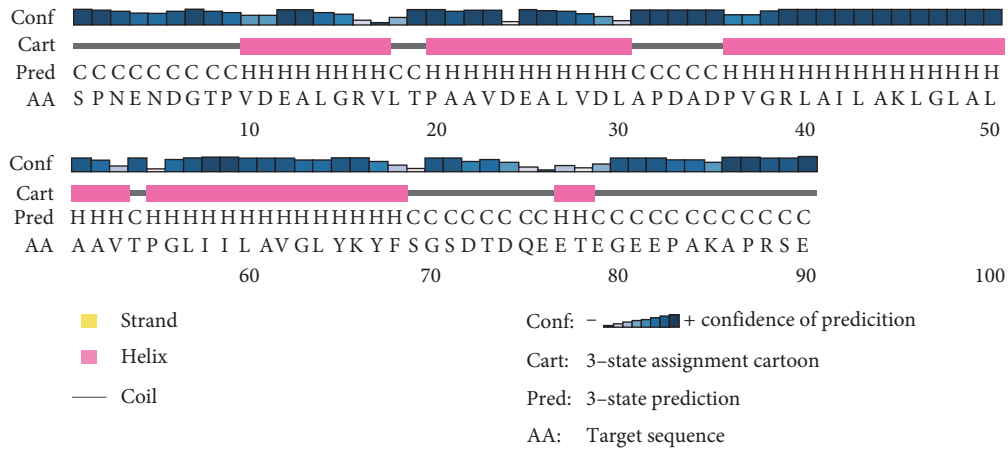
We expressed 3A recombinant protein with 6His tag in *E. coli* and purified by nickel resin affinity chromatography. Expression and purification of the 3A protein were assessed using SDS-PAGE and Western blot (Figure 1C,D). Results showed that the recombinant 3A protein had an approximate molecular weight of 17 kDa. Notably, the protein was predominantly soluble, and the purified 3A protein showed high purity.

3.2. Generation of MAb Against 3A Protein. The mice immunization strategy is shown in Figure 2A. Hybridoma cell supernatants were screened for specific antibodies using an IFA. Two hybridoma cell clones, AG4 and 2F3, secreted antibodies specifically recognized the SVA. After three rounds of subclone screening and multiple subclone passages, the ability of the hybridoma cells AG4 and 2F3 to secrete antibodies was maintained. The specificity of the mAbs was further validated using IFA and Western blot. IFA results showed that both mAb AG4 and 2F3 only reacted with SVA-infected BHK-21 cells instead of the uninfected cells (Figure 2B), indicating the high specificity of the mAbs. Additionally, Western blot analysis confirmed that mAb AG4 specifically reacted with the linear 3A recombinant protein, but mAb 2F3 could not (Figure 2C), which indicates that mAb 2F3 may recognize the conformational epitope on 3A protein. We also assessed the virus-neutralizing capacity of mAbs AG4 and 2F3. However, neither antibody showed neutralizing activity at a 1:2 dilution (against 50 TCID₅₀) (data not shown).

3.3. Identification of Epitopes Recognized by MAb AG4. To map the epitopes recognized by mAb AG4, eight truncated 3A proteins fused with GST were expressed, each with a 10 amino acid overlapping, and subjected to Western blot. MAb AG4 specifically recognized the recombinant protein



(A)



(B)

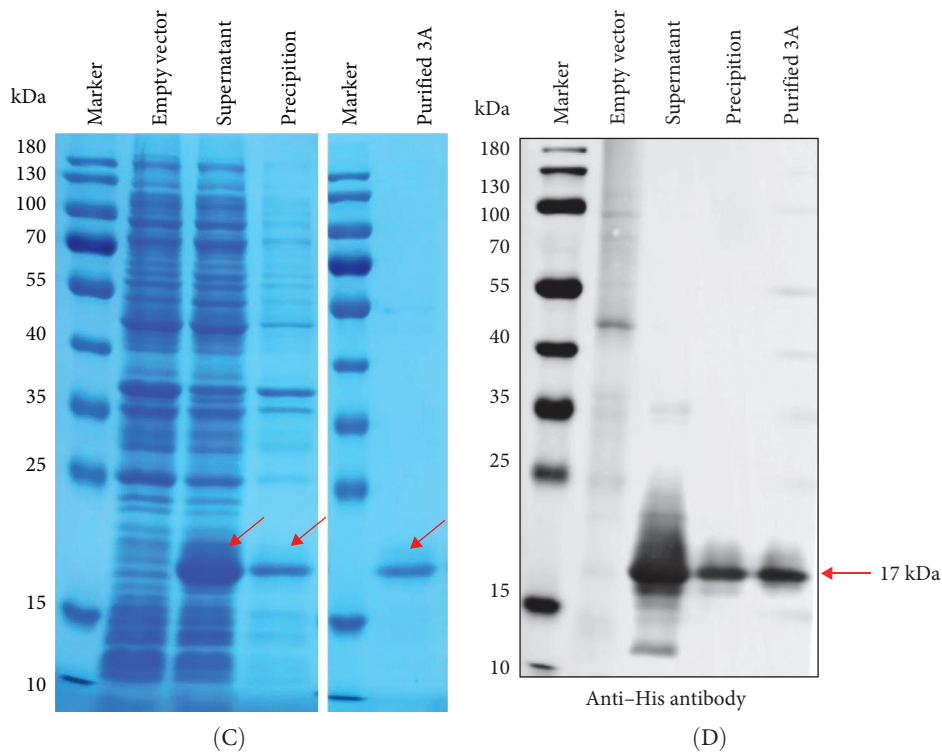


FIGURE 1: Characterization, expression, and purification of SVA 3A protein. (A) Analysis of antigenicity and hydrophilicity of 3A protein using Protean software. (B) The secondary structure of the 3A protein was analyzed by PSIPRED online software. (C, D) The expression in *E. coli* and purification of 3A protein were analyzed by SDS-PAGE (C) and Western blot (D).

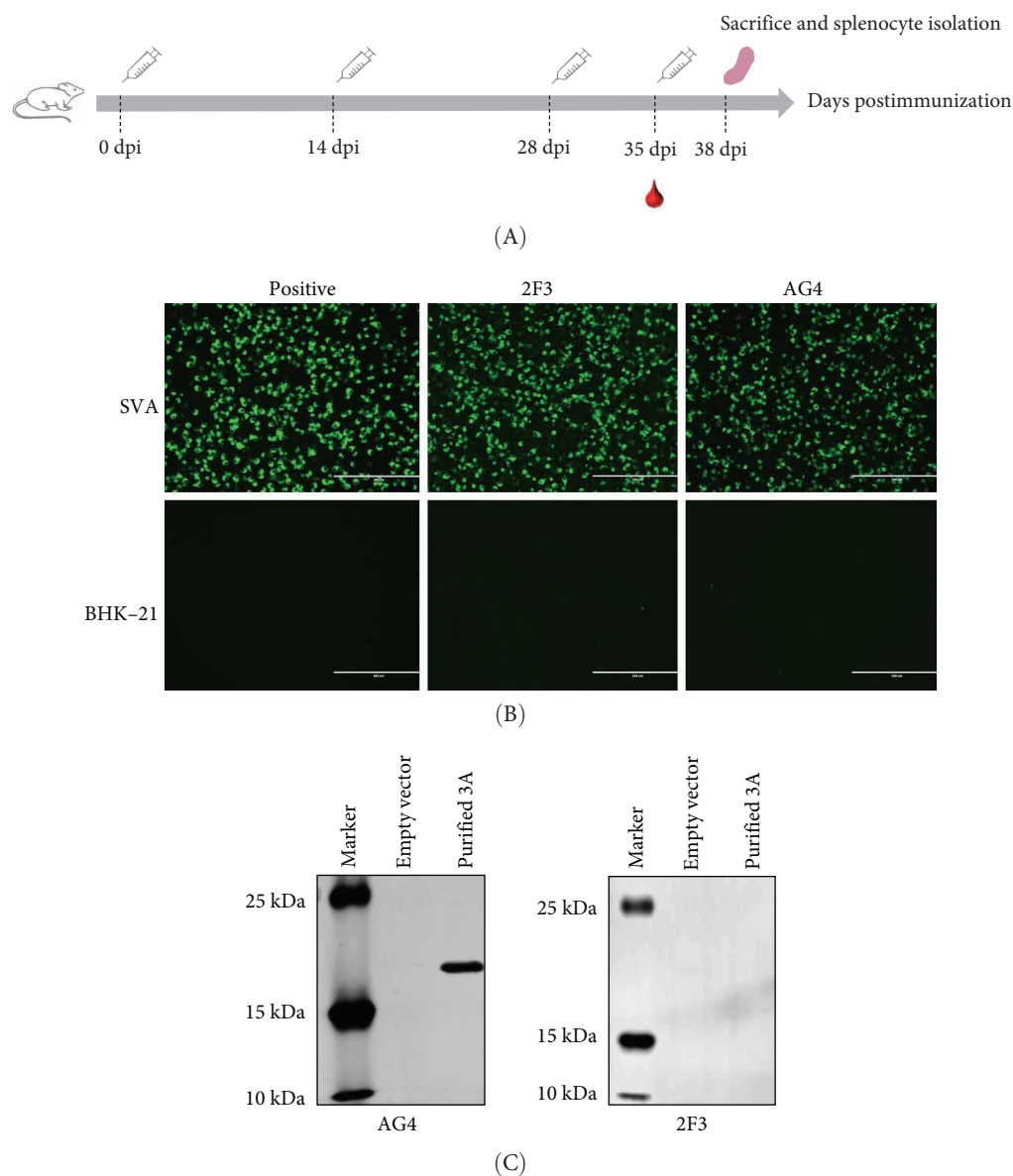


FIGURE 2: Preparation and functional analysis of mAbs. (A) Immunization protocol for mice. (B) BHK-21 cells were infected with SVA-WT at an MOI of 0.1. Cells were harvested and fixed at 24 hpi for IFA analysis using mAbs AG4 and 2F3 as primary antibody. (C) Western blot analysis of the reactivity of mAbs AG4 and 2F3 with the linear 3A protein.

GST-3A-1-20aa (Figure 3A). Additionally, we performed stepwise single amino acid truncations from the amino- and carboxyl-terminus of the 1–12 aa motif, respectively. Specifically, mAb AG4 recognized the 3AC1-6aa fusion peptide until truncation from the C-terminus to the sixth residue D (Figure 3B,C). However, mAb AG4 lost reactivity with the truncated protein lacking the fifth residue Asn. Similarly, truncation of the first amino acid Ser from the N-terminus also resulted in loss of reactivity with mAb AG4. These results indicated that the minimal epitope recognized by mAb AG4 is ¹SPNEND⁶.

To identify critical amino acids recognized by mAb AG4, we performed alanine scanning of ¹SPNEND⁶. Additionally, we mutated residue Ser¹ to Asn. The results showed that mutating Ser¹ to Ala or Asn did not affect mAb AG4 recognition

of the epitope, whereas mutating Asn³ to Ala resulted in loss of mAb AG4 reactivity (Figure 3D), indicating Asn³ is critical for the mAb AG4 recognition. Moreover, mutating Pro² and Asp⁶ to Ala significantly reduced mAb AG4 binding activity (Figure 3D), suggesting that Pro² and Asp⁶ are important for mAb AG4 binding.

3.4. MAb 2F3 Failed to React With SVA Mutant With 3A Protein C-Terminal Deletion. Given that mAb 2F3 did not react with the linear 3A recombinant protein (Figure 2C), it is hypothesized that the mAb 2F3 recognized epitope could be conformational. To determine the epitope recognized by 2F3, we first used the online tool Bepipred to predict B cell epitopes of the 3A protein. The results indicated that the 3A epitopes are primarily located at the N-terminus or the

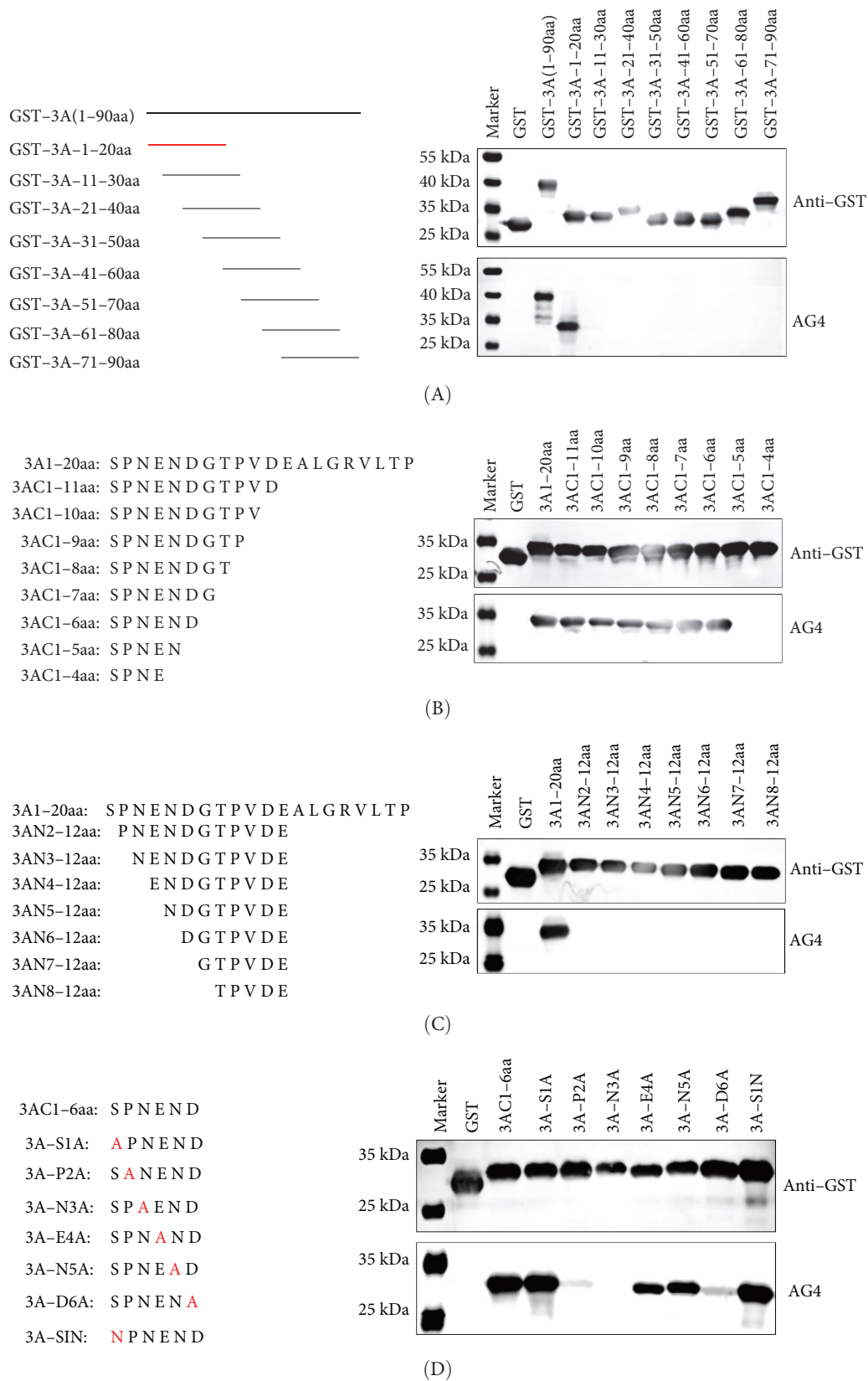


FIGURE 3: Epitope mapping of mAb AG4. (A) Eight overlapping truncated fragments of the 3A protein were expressed in *E. coli* BL21 and analyzed by Western blot using mAb AG4. (B, C) Identification of the minimal epitope recognized by mAb AG4. The 3A1-20aa fragment was sequentially truncated from the C-terminus (B) and N-terminus (C). (D) Alanine scanning was performed to identify the critical amino acids recognized by mAb AG4, as well as to mutate residue ¹S to ¹N.

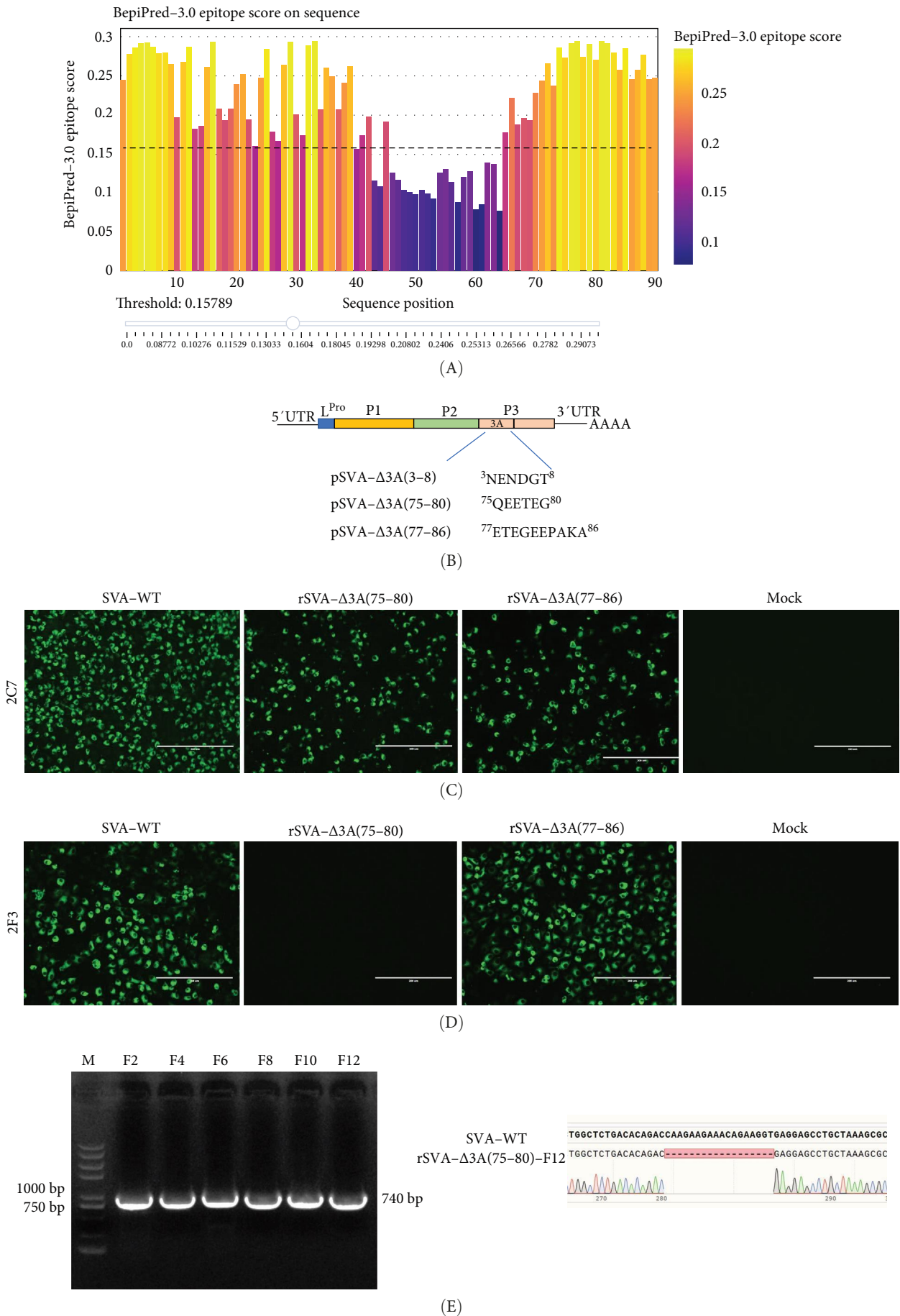


FIGURE 4: Continued.

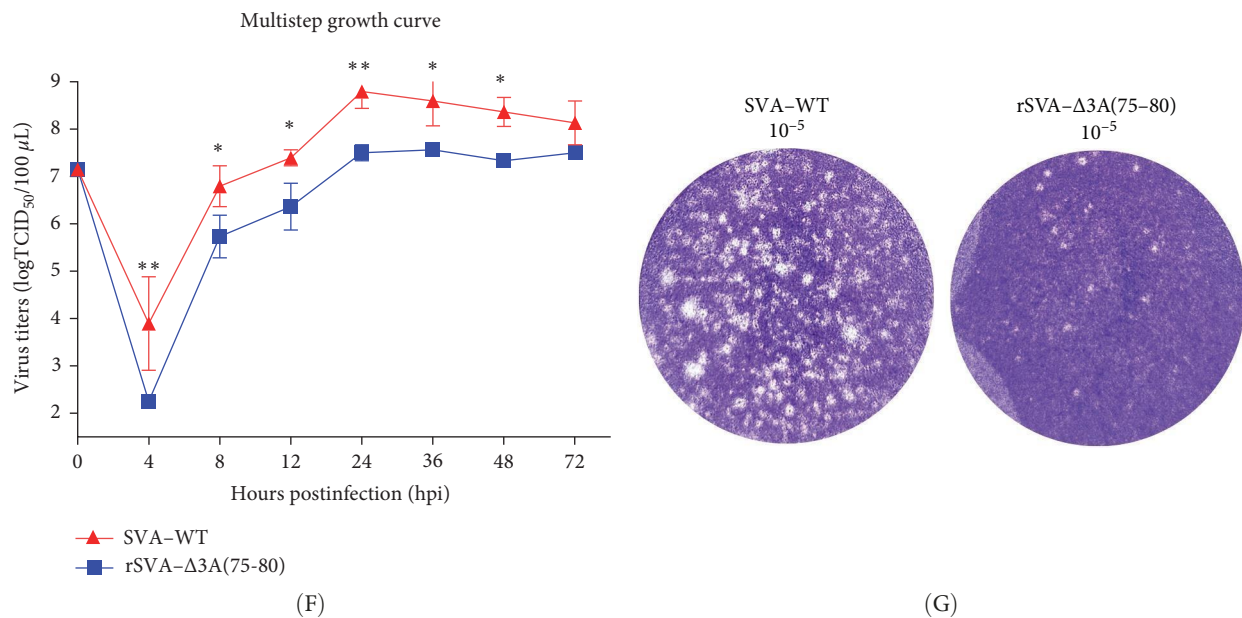


FIGURE 4: Construction of 3A epitope deletion mutants and epitope mapping of mAb 2F3. (A) The B cell epitope of SVA 3A was predicted using the BepiPred 3.0 tool. (B) Schematic diagram of the construction of 3A epitope deletion infectious clones. (C) The constructed infectious clones were transfected into BHK-21 cells for virus rescue. Only the pSVA-Δ3A(75-80) and pSVA-Δ3A(77-86) clones successfully rescued the virus, which were named rSVA-Δ3A(75-80) and rSVA-Δ3A(77-86), respectively. The infection of the rescued virus was detected by mAb 2C7. (D) To identify the epitope recognized by mAb 2F3, BHK-21 cells were infected with the rescued epitope deletion viruses rSVA-Δ3A(75-80) and rSVA-Δ3A(77-86) at an MOI of 0.1. Cells were harvested and fixed at 12 hpi for IFA using mAb 2F3. (E) The rSVA-Δ3A(75-80) virus was serially passaged 12 times in BHK-21 cells, and the genetic stability analysis of the epitope deletion virus rSVA-Δ3A(75-80) was conducted. Nucleic acids were extracted and PCR amplified from passages 2, 4, 6, 8, 10, and 12. The PCR product from the 12th passage was sequenced for validation. (F) Growth curve of SVA WT and rSVA-Δ3A. BHK-21 cells were infected with SVA-WT and rSVA-Δ3A(75-80) at an MOI of 0.01. Samples were collected at various time points postinfection and titrated on BHK-21 cells. The data were presented as the means \pm SD ($n = 3$ biological replicates). p values were calculated using two-way analyses of variance as * $p < 0.05$ and ** $p < 0.01$. (G) Plaque morphologies of SVA-WT and the epitope deletion mutant rSVA-Δ3A(75-80).

C-terminus (Figure 4A). Based on these predictions, several consecutive amino acids with high antigenicity indices from both the N-terminus and C-terminus were selected as potential dominant antigenic epitopes. These regions were then used to construct infectious clones of 3A epitope deletion mutants: pSVA-Δ3A(3-8), pSVA-Δ3A(75-80), and pSVA-Δ3A(77-86) (Figure 4B). The constructed infectious clones were transfected into BHK-21 cells to rescue the SVA 3A-deletion mutants. The results showed that pSVA-Δ3A(3-8) was lethal, but pSVA-Δ3A(75-80) and pSVA-Δ3A(77-86) were successfully rescued and were designated as rSVA-Δ3A(75-80) and rSVA-Δ3A(77-86), respectively (Figure 4C). IFA using mAb 2F3 as the primary antibody revealed that mAb reacted with the epitope deletion mutant rSVA-Δ3A(77-86) but not rSVA-Δ3A(75-80) (Figure 4D), indicating that the ⁷⁵QEETEG⁸⁰ deletion is the essential epitope recognized by mAb 2F3. The overlapping sequence between rSVA-Δ3A(75-80) and rSVA-Δ3A(77-86) is ⁷⁷EETEG⁸⁰; thus, the nonoverlapping motif is ⁷⁵QE⁷⁶. MAb 2F3 failed to react with SVA mutant with ⁷⁵QE⁷⁶ deletion, indicating ⁷⁵QE⁷⁶ is the crucial motif for mAb 2F3 recognition.

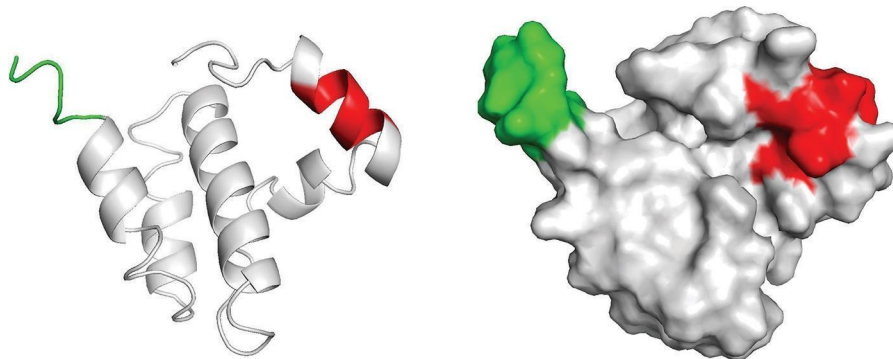
Additionally, we assessed the genetic stability and replication dynamics of the deletion mutant rSVA-Δ3A(75-80). After 12 serial passages, no additional amino acid deletions, insertions, or mutations were observed (Figure 4E), indicating

that pSVA-Δ3A(75-80) was genetically stable. Multistep growth curve results showed that the replication dynamics of the deletion mutant were similar to those of SVA-WT, though its replication capacity was approximately one log lower than that of SVA-WT (Figure 4F). Moreover, after infecting BHK-21 cells with the same dilution of virus for 48 h, the number and size of plaques produced by epitope deletion mutant rSVA-Δ3A(75-80) were significantly smaller than those produced by SVA-WT (Figure 4G), further demonstrating that the replication ability and growth rate of the deletion mutant were slower compared to SVA-WT.

3.5. The Identified Epitopes Are Highly Conserved and Surface-Located in the 3A Proteins. Sequence alignment of the 3A protein from different SVA isolates showed that the epitope ¹SPNEND⁶ and ⁷⁵QEETEG⁸⁰ are highly conserved, except for a single amino acid substitution (Figure 5A). The 3D structure of the 3A protein was predicted using the I-TASSER server and visualized for analysis. The results revealed that the epitope ¹SPNEND⁶ is situated in a random coil region, while the epitope ⁷⁵QEETEG⁸⁰ is located within an α -helix. Both epitopes are positioned on the surface of the 3A protein (Figure 5B). Furthermore, we aligned the SVA 3A protein sequence with 3A homologs from representative picornaviruses, including FMDV, enterovirus 71 (EV71),

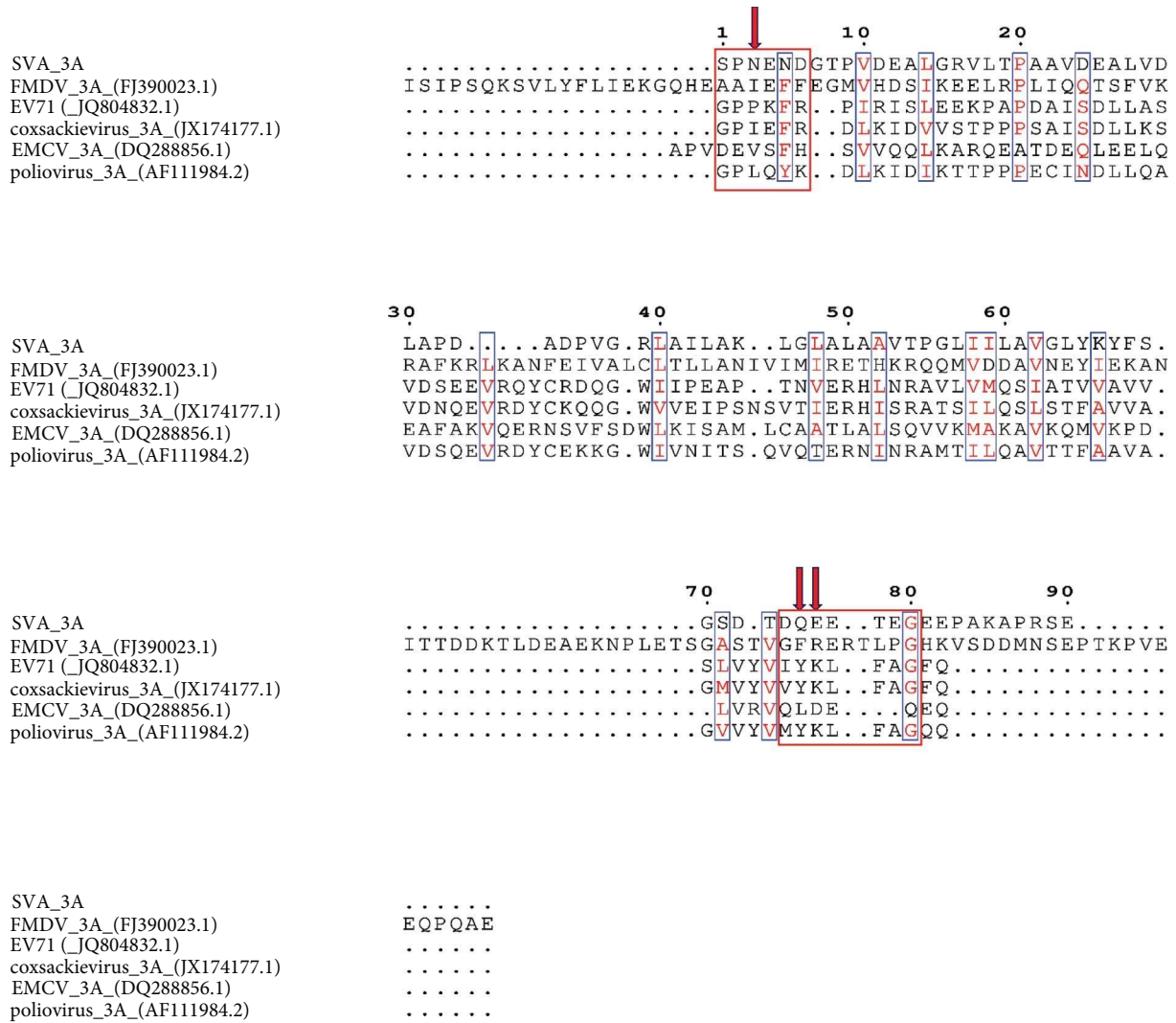
SVA/HLJ/CHA/2016	1	10	70	80
pKS15-01	SPNEND	GTPV	SDTDQEETE	G
KS15-01	SPNEND	DTPV	SDTDQEETE	S
SVA/USA/MN/004/2015	SPNEND	DTPV	SDTDQEETE	S
US-15-41901SD	NPNEND	DTPV	SDTDQEETE	S
SVA/USA/MN/013/2016	SPNEND	DTPV	SDTDQEETE	S
SVA/USA/MN/007/2015	SPNEND	DTPV	SDTDQEETE	S
SVA/US/CA/17-97-3D/2017	SPNEND	DTPV	SDTDQEETE	S
SVA/US/CA/17-94-9D/2017	SPNEND	DTPV	SDTDQEETE	S
CH-HuB-2017	SPNEND	DTPV	SDTDQEETE	T
SVA/US/CA/17-43-3D/2017	SPNEND	DTPV	SDTDQEETE	T
SVA-GDSZ-2018	SPNEND	DTPV	SDTDQEETE	S
HN01-2017	SPNEND	NTSV	SDTDQEETE	S
SVA/US/CA/17-57-11D/2017	SPNEND	DTPV	SDTDQEETE	T
HS-03	SPNEND	DLV	SDADQEETE	T
HBWH-JX2017	SPNEND	DTPV	SDTDQEETE	S
US-15-41901SD	NPNEND	DTPV	SDTDQEETE	S
Colombia/2016	SPNEND	DTPV	SDTDQEETE	S
SVA/US/SVV-001-P3/2002	SPNEND	DTPV	SDADQEETE	S

(A)



(B)

FIGURE 5: Continued.



(C)

FIGURE 5: Structural analysis and multiple sequence alignment of SVA 3A. (A) Sequence alignment analysis of the identified epitopes was performed using MEGA 7.0 software. The sequence alignment of the epitope ¹SPNEND⁶ among different SVA isolates (left) and the alignment of the epitope ⁷⁵QEETEG⁸⁰ among different SVA isolates (right). (B) The detailed positions of the 3A protein epitopes ¹SPNEND⁶ (red) and ⁷⁵QEETEG⁸⁰ (green) were analyzed, respectively. (C) Sequence alignment analysis of 3A proteins of different picornaviruses. The red arrows indicate the key amino acids identified. The red boxes represent the epitope ¹SPNEND⁶ and ⁷⁵QEETEG⁸⁰, respectively.

encephalomyocarditis virus (EMCV), poliovirus, and coxsackievirus. The results demonstrated low sequence homology between SVA 3A and other picornaviral 3A proteins. Although the G⁸⁰ residue within the ⁷⁵QEETEG⁸⁰ epitope showed partial overlap in some viruses, the critical residues (Asn³ in ¹SPNEND⁶ and the ⁷⁵QE⁷⁶ motif in ⁷⁵QEETEG⁸⁰) were entirely non-conserved (Figure 5C). This lack of conservation suggests a minimal risk of cross-reactivity.

4. Discussion

SVA is affecting the swine industry in many countries and regions around the world, undergoing genetic evolution and viral recombination [20, 21]. Despite extensive research into potential vaccine candidates, no commercial vaccine is currently available, and the lack of differentiating infected from

vaccinated animals (DIVA) strategies, complicating disease control and surveillance [22, 23]. FMDV, a member of the *Picornaviridae* family, can tolerate certain amino acid deletions in its 3A protein [24, 25], aiding the development of DIVA marker vaccines [16]. Additionally, the 3AB nonstructural protein, a precursor to 3A, elicits early and sustained antibody responses that are detectable as early as 7-day post-infection [17]. This characteristic of immunogenicity and modifiability make 3A protein an ideal target for early diagnosis and development of DIVA-based SVA vaccine.

In this study, we expressed and purified SVA 3A protein to prepare mAbs, obtaining mAbs AG4 and 2F3. AG4 specifically binds to the linear epitope ¹SPNEND⁶ on 3A protein, with Asn3 identified as a critical residue for antibody binding. Although an partial overlapping epitope (⁵NDDTPVDEALGR¹⁶) has been reported [26], our work provides a refined characterization of

the AG4-binding epitope, resolving its precise boundaries (¹SPNEND⁶) and pinpointing Asn³ as a key recognition site. This difference in comparison to the previously described regions indicates that the epitopes we have identified are different from each other. Furthermore, we identified a novel conformational epitope, ⁷⁵QEETEG⁸⁰, where the ⁷⁵QE⁷⁶ motif is essential for recognition by 2F3. Sequence alignment and structural analysis revealed that both epitopes are highly conserved among different SVA isolates and are exposed on the surface of the 3A protein (Figure 5A,B), highlighting their significance as antigenic sites.

The FMDV 3A protein is crucial for viral virulence and host specificity, with specific deletions restricting replication in bovine cells and attenuating virulence [27, 28]. In many small RNA viruses, the 3A protein forms the viral replication complex, promoting replication [29–31]. The predicted SVA 3A protein (Figure 1A,B) contains an N-terminal domain, a central transmembrane hydrophobic domain, and a C-terminal domain similar to FMDV 3A protein [32, 33]. Although the function of the C-terminal domain in FMDV remains unclear, the deletion of amino acids 75–80 in rSVA-Δ3A(75-80) resulted in reduced replication and growth capacity compared to SVA-WT (Figure 4F,G), indicating the C-terminus region of 3A protein influences the replication of SVA. The specific mechanism requires further investigation. Importantly, mAb 2F3 did not react with virus rSVA-Δ3A(75-80) (Figure 4D), indicating the potential of ⁷⁵QEETEG⁸⁰ deletion as a specific marker to distinguish between SVA-WT and rSVA-Δ3A(75-80).

This study prepared two mAbs against the 3A protein and identified their antigenic epitopes, laying the foundation for further exploration of the 3A protein's function and potential targets for differential diagnostic methods. The rSVA-Δ3A(75-80) with deleted epitope does not react with the mAb 2F3, potentially making it a negative marker to distinguish between wild-type virus infection and vaccine immunity. In future studies, we will validate the potential of the epitope-deleted virus rSVA-Δ3A(75-80) as a DIVA-based vaccine candidate and analyze vaccine-induced immunity from wild-type virus infection in vivo and further develop differential diagnostic tools.

Data Availability Statement

The data that support the findings of this study are available from the corresponding author upon reasonable request.

Ethics Statement

The animal experiment was conducted following the recommendation in the Guide for the Care and Use of Laboratory Animals of the Ministry of Science and Technology of the People's Republic of China. The protocol was approved by the Committee on the Ethics of Animal Experiments of the Harbin Veterinary Research Institute (HVRI) of the Chinese Academy of Agricultural Sciences (CAAS) and the Animal Ethics Committee of Heilongjiang Province, China (Permission number: 220908-01-GR).

Conflicts of Interest

The authors declare no conflicts of interest.

Author Contributions

Liang Meng and Xiao-Xiao Tian contributed equally to this work.

Funding

The study was supported by grants from the Heilongjiang Provincial Key Laboratory of Veterinary Immunology (JD22A023) and the National Natural Science Foundation of China to Fan-Dan Meng (32002249).

Acknowledgments

The study was supported by grants from the Heilongjiang Provincial Key Laboratory of Veterinary Immunology (JD22A023) and the National Natural Science Foundation of China to Fan-Dan Meng (32002249).

Supporting Information

Additional supporting information can be found online in the Supporting Information section. (*Supporting Information*) Table S1. The sequence of primers. Table S2. The sequence of primers.

References

- [1] L. M. Hales, N. J. Knowles, P. S. Reddy, L. Xu, C. Hay, and P. L. Hallenbeck, "Complete Genome Sequence Analysis of Seneca Valley Virus-001, a Novel Oncolytic Picornavirus," *Journal of General Virology* 89, no. 5 (2008): 1265–1275.
- [2] J. Segalés, D. Barcellos, A. Alfieri, E. Burrough, and D. Marthaler, "Senecavirus A: An Emerging Pathogen Causing Vesicular Disease and Mortality in Pigs?" *Veterinary Pathology* 54, no. 1 (2016): 11–21.
- [3] F. A. Vannucci, D. C. Linhares, D. E. Barcellos, H. C. Lam, J. Collins, and D. Marthaler, "Identification and Complete Genome of Seneca Valley Virus in Vesicular Fluid and Sera of Pigs Affected With Idiopathic Vesicular Disease, Brazil," *Transboundary and Emerging Diseases* 62, no. 6 (2015): 589–593.
- [4] P. Canning, A. Canon, J. L. Bates, et al., "Neonatal Mortality, Vesicular Lesions and Lameness Associated With Senecavirus A in a U.S. Sow Farm," *Transboundary and Emerging Diseases* 63, no. 4 (2016): 373–378.
- [5] T. Pasma, S. Davidson, and S. L. Shaw, "Idiopathic Vesicular Disease in Swine in Manitoba," *Canadian Veterinary Journal-Revue Veterinaire Canadienne* 49, no. 1 (2008): 84–85.
- [6] R. A. Leme, E. Zotti, B. K. Alcântara, et al., "Senecavirus A: An Emerging Vesicular Infection in Brazilian Pig Herds," *Transboundary and Emerging Diseases* 62, no. 6 (2015): 603–611.
- [7] S. k. Corner, "Seneca Valley Virus and Vesicular Lesions in a Pig With Idiopathic Vesicular Disease," *Journal of Veterinary Science and Technology* 3, no. 6: 123.
- [8] J. Arzt, M. R. Bertram, L. T. Vu, et al., "First Detection and Genome Sequence of Senecavirus A in Vietnam," *Microbiology Resource Announcements* 8, no. 3 (2019): e01247-18.

- [9] K. Saeng-chuto, P. Rodtian, G. Temeeyasen, M. Wegner, and D. Nilubol, "The First Detection of Senecavirus A in Pigs in Thailand, 2016," *Transboundary and Emerging Diseases* 65, no. 1 (2018): 285–288.
- [10] Z. Wang, X. Zhang, R. Yan, et al., "Emergence of a Novel Recombinant Seneca Valley Virus in Central China, 2018," *Emerging Microbes & Infections* 7, no. 1 (2018): 180.
- [11] M. Strauss, N. Jayawardena, E. Sun, R. A. Easingwood, L. N. Burga, and M. Bostina, "Cryo-Electron Microscopy Structure of Seneca Valley Virus Procapsid," *Journal of Virology* 92, no. 6 (2018): e01927-17.
- [12] W. Yang, D. Li, Y. Ru, et al., "Foot-and-Mouth Disease Virus 3A Protein Causes Upregulation of Autophagy-Related Protein LRRC25 To Inhibit the G3BP1-Mediated RIG-Like Helicase-Signaling Pathway," *Journal of Virology* 94, no. 8 (2020): e02086-19.
- [13] H. Zhou, M. Sun, S. Su, et al., "Identification of a Linear B-Cell Epitope on the "Puff" Loop of the Senecavirus A VP2 Protein Involved in Receptor Binding," *Frontiers in Microbiology* 15 (2024): 1387309.
- [14] H. Fan, H. Zhu, S. Li, et al., "Identification of Linear B Cell Epitopes on VP1 and VP2 Proteins of Senecavirus A (SVA) Using Monoclonal Antibodies," *Veterinary Microbiology* 247 (2020): 108753.
- [15] M. Chen, L. Chen, J. Wang, C. Mou, and Z. Chen, "Identification of a B-Cell Epitope in the VP3 Protein of Senecavirus A," *Viruses* 13, no. 11 (2021): 2300.
- [16] V. V. Dhanesh, M. Hosamani, S. H. Basagoudanavar, et al., "Immunogenicity and Protective Efficacy of 3A Truncated Negative Marker Foot-and-Mouth Disease Virus Serotype A Vaccine," *Applied Microbiology and Biotechnology* 104, no. 6 (2020): 2589–2602.
- [17] J. Yan, Y. Gao, J. Li, et al., "The Establishment and Application of Indirect 3AB-ELISA for the Detection of Antibodies Against Senecavirus A," *Viruses* 15, no. 4 (2023): 861.
- [18] H. Wang, C. Li, B. Zhao, et al., "Complete Genome Sequence and Phylogenetic Analysis of Senecavirus A Isolated in Northeast China in 2016," *Archives of Virology* 162, no. 10 (2017): 3173–3176.
- [19] P. Huang, S. Y. Yu, and C. W. Ke, "Stepwise Prediction and Statistical Screening: B-cell Epitopes on Neuraminidase of Human Avian H5N1 Virus," *Chinese Science Bulletin* 53, no. 23 (2008): 3642–3647.
- [20] Z. Guo, X.-X. Chen, H. Ruan, S. Qiao, R. Deng, and G. Zhang, "Isolation of Three Novel Senecavirus A Strains and Recombination Analysis Among Senecaviruses in China," *Frontiers in Veterinary Science* 7 (2020): 2.
- [21] L. R. Joshi, K. A. Mohr, D. Gava, et al., "Genetic Diversity and Evolution of the Emerging Picornavirus *Senecavirus A*." *The Journal of general virology* 101, no. 2 (2020): 175–187.
- [22] F. Yang, Z. Zhu, W. Cao, et al., "Immunogenicity and Protective Efficacy of an Inactivated Cell Culture-Derived Seneca Valley Virus Vaccine in Pigs," *Vaccine* 36, no. 6 (2018): 841–846.
- [23] A. Buckley and K. Lager, "Efficacy of an Inactivated Senecavirus A Vaccine in Weaned Pigs and Mature Sows," *Vaccine* 40, no. 12 (2022): 1747–1754.
- [24] C. Stenfeldt, J. Arzt, J. M. Pacheco, et al., "A Partial Deletion Within Foot-and-Mouth Disease Virus Non-Structural Protein 3A Causes Clinical Attenuation in Cattle But Does Not Prevent Subclinical Infection," *Virology* 516 (2018): 115–126.
- [25] J. M. Pacheco, T. M. Henry, V. K. O'Donnell, J. B. Gregory, and P. W. Mason, "Role of Nonstructural Proteins 3A and 3B in Host Range and Pathogenicity of Foot-and-Mouth Disease Virus," *Journal of Virology* 77, no. 24 (2003): 13017–13027.
- [26] X. H. Ling, B. Zhang, H. J. Ren, et al., "Preparation and Epitope Identification of a Novel Monoclonal Antibody Against 3A Protein of Senecavirus A," *Veterinary Microbiology* 303 (2025): 110442.
- [27] C. W. Beard and P. W. Mason, "Genetic Determinants of Altered Virulence of Taiwanese Foot-and-Mouth Disease Virus," *Journal of Virology* 74, no. 2 (2000): 987–991.
- [28] J. I. Núñez, E. Baranowski, N. Molina, et al., "A Single Amino Acid Substitution in Nonstructural Protein 3A Can Mediate Adaptation of Foot-and-Mouth Disease Virus to the Guinea Pig," *Journal of Virology* 75, no. 8 (2001): 3977–3983.
- [29] J. Tang, S. W. Abdullah, P. Li, et al., "Heat Shock Protein 60 is Involved in Viral Replication Complex Formation and Facilitates Foot and Mouth Virus Replication by Stabilizing Viral Nonstructural Proteins 3A and 2C," *MBio* 13, no. 5 (2022): 2022–e0143422.
- [30] K. Ishikawa-Sasaki, J. Sasaki, K. Taniguchi, and K. Kirkegaard, "A Complex Comprising Phosphatidylinositol 4-Kinase III β , ACBD3, and Aichi Virus Proteins Enhances Phosphatidylinositol 4-Phosphate Synthesis and is Critical for Formation of the Viral Replication Complex," *Journal of Virology* 88, no. 12 (2014): 6586–6598.
- [31] N. Y. Hsu, O. Ilnytska, G. Belov, et al., "Viral Reorganization of the Secretory Pathway Generates Distinct Organelles for RNA Replication," *Cell* 141, no. 5 (2010): 799–811.
- [32] M. González-Magaldi, M. A. Martín-Acebes, L. Kremer, and F. Sobrino, "Membrane Topology and Cellular Dynamics of Foot-and-Mouth Disease Virus 3A Protein," *PLoS One* 9, no. 9 (2014): e106685.
- [33] S. Forss, K. Strebel, E. Beck, and H. Schaller, "Nucleotide Sequence and Genome Organization of Foot-and-Mouth Disease Virus," *Nucleic Acids Research* 12, no. 16 (1984): 6587–6601.